Geologie en Mijnbouw 67: 379–395 (1988)

Activity diagrams for the MgO-Na_2O-K_2O-SiO_2-Al_2O_3-H_2O-HCl system in the temperature range 298 to 623 K and 1 bar pressure: application to the 1900 Ma phlogopite-Mg-chlorite-sericite schists of W. Bergslagen, Sweden

A.W. Jasiński
Institute of Inorganic Chemistry and Metallurgy of Rare Elements, Technical University of Wroclaw, Wybrzeze Wyspiańskiego 27, 50-370 Wroclaw, Poland

Received 26 May 1987; accepted in revised form 26 June 1987

Key words: thermodynamic calculations, phlogopite stability, reaction constants, applications, hydrothermal alteration, Bergslagen

Abstract

Both 2- and 3-dimensional activity diagrams for the MgO-Na_2O-K_2O-SiO_2-Al_2O_3-H_2O-HCl system at temperatures of 298 to 623 K and 1 bar pressure are presented, showing the stability fields and volumes of phlogopite, Mg-chlorite, muscovite, paragonite, microcline, albite, kaolinite, and Mg-, Na-, and K-montmorillonite. Additionally, the expressions of reaction constants also contain the pressure term. The geological application of these diagrams to geochemical interpretation is briefly discussed in relation to the formation of 1900 Ma phlogopite-Mg-chlorite-sericite-quartz rocks in W. Bergslagen, Central Sweden.

Introduction

Activity diagrams illustrating the stability areas of mineral phases are very useful tools for the assessment and geochemical interpretation of naturally occurring assemblages of minerals. Such diagrams may also be used to indicate suitable areas for experimental studies.

Field studies in the Bergslagen ore province of Central Sweden have demonstrated the importance of hydrothermal alteration processes in the felsic volcanics hosting major ore bodies (Oen et al., 1982; Frietsch, 1982; Lagerblad & Gorbatschev, 1985; Oen, 1987). Baker and De Groot (1983) and Jasiński et al. (1985) discuss Mg-enrichment and the physico-chemical conditions of the formation of Mg-chlorite-mica-quartz schist in felsic pyroclastics in the Hjulsjö area, linking the growth of Mg-chlorite to seawater – rock interaction. Similar processes have been discussed by Lagerblad & Gorbatschev (1985), Ripa (1988) and Trägårdh (1988).

This study was initiated as a result of the discovery of Mg-rich alteration zones SE of Hällefors with a phlogopite-sericite – quartz paragenesis (Linthout, 1983). This investigation into the MgO-Na_2O-K_2O-SiO_2-Al_2O_3-H_2O-HCl system supplements the previous work of Helgeson et al. (1969), which did not include the stability fields of phlogopite.

Method of calculation

The calculations are based primarily upon currently available data (Table 1) from Helgeson et al. (1978) and Robie et al. (1978). The thermodynamic data for montmorillonites and illite are only approximations, based partly on the suggestions of Tardy & Garrels (1974), on naturally existing mineral assemblages described in the literature, and the demands imposed by graphical representation. Volume values for these minerals are based upon approximations of entropies, as proposed by Helgeson et al. (1978).

Table 2 presents all the reactions used to construct the activity diagrams, including the pressure term in the expressions of reaction constant:

$(\log K_{T,P} = -\triangle H_{298,1}/2{,}303\ RT + \triangle S_{298,1}/2{,}303\ R - (P-1)\ \triangle V_{298,1}/RT)$ where:
$\triangle H_{298,}1$, $\triangle S_{298,1}$ and $\triangle V_{298,1}$

represent the change of enthalpy, entropy and volume, respectively of a given reaction at 298 K and 1 bar; T, p are temperature in degrees Kelvin, and pressure in bars; R represents the gas constant.

In all calculations it is assumed that:
- H_2O refers to liquid water with a $H_2O = 1$;
- activities of all solid phasies are 1;
- $\triangle Cp$ (change of the heat capacity) and $\triangle V$ are temperature independent; and
- the system is quartz-saturated.

As much of available data and thus some of the approximations are subject to large uncertainties, the diagrams should be regarded as provisional representations of chemical equilibria in natural systems.

Montmorillonites are illustrated here by their Mg, Na and K end-members for simplicity, and to depict areas of relatively higher contributions of a respective cation. Illite should be considered as an additional option, primarily when K- and Mg-montmorillonite areas of stability are taken into account.

The thermodynamic relations and methods in the construction of activity diagrams have been presented in several sources (e.g. Garrels & Christ,

Table 1. Thermodynamic data for 298 K, p = lb used in the calculations.

mineral/ion	$\triangle G°$ form cal/mol	$\triangle H°$ form cal/mol	S° form cal/mol	V° cm^3
$H_2O_{(liq)}$	− 56688	− 68315	16,71	18,069
SiO_2	− 204646	− 217650	9,88	22,688
MgO	− 136086	− 143800	6,44	11,248
K_2O	− 77056	− 86800	22,5	40,38
Na_2O	− 89883	− 99140	17,935	25,00
Al_2O_3	− 374824	− 397145	12,18	25,575
$Mg_5Al\ (AlSi_3O_{10})\ (OH)_8$ (Mg-chlorite)	− 1957101	− 2113197	106,5	211,5
$NaAlSi_3O_8$ (albite)	− 886308	− 939680	49,51	100,25
$KAlSi_3O_8$ (K-feldspar)	− 895374	− 949188	51,13	108,741
$Al_2Si_2O_5\ (OH)_4$ (kaolinite)	− 982221	− 905614	48,53	99,52
$KAl_2\ (AlSi_3O_{10})\ (OH)_2$ (musc.)	− 1336301	− 1427408	68,8	140,71
$KMg_3\ (AlSi_3O_{10})\ (OH)_2$ (phlogop.)	− 1396187	− 1488067	76,1	149,66
$Al_2Si_4O_{10}\ (OH)_2$ (pyrophyl.)	− 1255997	− 1345313	57,2	126,6
$NaAl_2\ (AlSi_3O_{10})\ (OH)_2$ (paragon.)	− 1326012	− 1416963	66,4	132,53
$K_{0,33}Al_2, {}_{33}Si_3, {}_{67}O_{10}\ (OH)_2$ (K-mont)	− 1282855	− 1370500	68,47	153,4
$Mg_{0,167}Al_2, {}_{33}Si_3, {}_{67}O_{10}\ (OH)_2$ (Mg-mont)	− 1278333	− 1366750	62,08	132,88
$Na_{0,33}Al_2, {}_{33}Si_3, {}_{67}O_{10}\ (OH)_2$ (Na-mont)	− 1280456	− 1369672	62,13	127,44
$K_{0,6}Mg_{0,25}Al_2, {}_3Si_3, {}_{67}O_{10}\ (OH)_2$ (illite)	− 1304519	− 1396826	57,99	92,45
Na^+ (aq)	− 62597	− 57433	13,96	
K^+ (aq)	− 67579	− 60270	24,38	
Mg^{++} (aq)	− 108725	− 111580	32,98	

Table 2. Reactions used to construct curves in figs 1–2. (Numbers of lines refer to numbers in figures.)

No.	reaction; $\log K$; $\log \frac{a Me^{+n}}{a^n_{H+}}$
1	$2KAlSi_3O_8 + H_2O + 2H^+ \rightleftarrows Al_2Si_2O_5(OH)_4 + 2K^+ + 4SiO_2$ $\log K = \frac{1456}{T} + 3{,}874 + 0{,}236\frac{(P-1)}{T}$; $\log\frac{aK^+}{aH^+} = 0{,}5 \log K$
2	$Mg_5Al_2Si_3O_{10}(OH)_8 + 10H^+ \rightleftarrows Al_2Si_2O_5(OH)_4 + 5Mg^{++} + SiO_2 + 7H_2O$ $\log K = \frac{26823}{T} - 21{,}403 - 0{,}194\frac{(P-1)}{T}$; $\log\frac{aMg^{++}}{a^2H^+} = 0{,}2 \log K$
3	$2NaAlSi_3O_8 + 2H^+ + H_2O \rightleftarrows Al_2Si_2O_5(OH)_4 + 2Na^+ + 4SiO_2$ $\log K = \frac{4372}{T} + 0{,}062 + 0{,}148\frac{(P-1)}{T}$; $\log\frac{aNa^+}{aH^+} = 0{,}5 \log K$
4	$3Mg_5Al_2Si_3O_{10}(OH)_8 + 6K^+ + 24H^+ + 9SiO_2 \rightleftarrows 24H_2O + 15Mg^{++} + 6KAlSi_3O_8$ $\log K = \frac{76101}{T} - 75{,}831 - 1{,}292\frac{(P-1)}{T}$; $\log\frac{aK^+}{aH^+} = -0{,}167 \log K + 2{,}5 \log\frac{aMg^{++}}{a^2H^+}$
5	$2{,}3\,KAlSi_3O_8 + 0{,}25\,Mg^{++} + 0{,}4\,H_2O + 1{,}2\,H^+ \rightleftarrows K_{0,6}Mg_{0,25}Al_{2,3}Si_{3,5}O_{10}(OH)_2 + 1{,}7K^+ + 3{,}4SiO_2$ $\log K = \frac{204}{T} + 3{,}702 + 0{,}458\frac{(P-1)}{T}$; $\log\frac{aK^+}{aH^+} = 0{,}588 \log K + 0{,}147 \log\frac{aMg^{++}}{a^2H^+}$
6	$1{,}15Al_2Si_2O_5(OH)_4 + 1{,}2SiO_2 + 0{,}25Mg^{++} + 0{,}6K^+ \rightleftarrows 0{,}75H_2O + K_{0,6}Mg_{0,2}Al_{2,3}Si_{3,5}O_{10}(OH)_2 + 1{,}1H^+$ $\log K = \frac{1470}{T} - 0{,}753 + 0{,}186\frac{(P-1)}{T}$; $\log\frac{aK^+}{aH^+} = -1{,}667 \log K - 0{,}417 \log\frac{aMg^{++}}{a^2H^+}$
7	$1{,}15Mg_5Al_2Si_3O_{10}(OH)_2 + 0{,}05SiO_2 + 0{,}6K^+ + 10{,}4H^+ \rightleftarrows 5{,}5Mg^{++} + 8{,}8H_2O + K_{0,6}Mg_{0,25}Al_{2,3}Si_{3,5}O_{10}(OH)_2$ $\log K = \frac{29376}{T} - 25{,}366 - 0{,}037\frac{(P-1)}{T}$; $\log\frac{aK^+}{aH^+} = 9{,}167 \log\frac{aMg^{++}}{a^2H^+}$
8	$KAlSi_3O_8 + Na^+ \rightleftarrows NaAlSi_3O_8 + K^+$ $\log K = -\frac{1458}{T} + 1{,}897 + 0{,}044\frac{(P-1)}{T}$; $\log\frac{aK^+}{aH^+} = \log K + \log\frac{aNa^+}{aH^+}$
9	$Mg_5Al_2Si_3O_{10}(OH)_8 + 2Na^+ + 3SiO_2 + 8H^+ \rightleftarrows 5Mg^{++} + 8H_2O + 2NaAlSi_3O_8$ $\log K = \frac{22502}{T} - 21{,}516 - 0{,}342\frac{(P-1)}{T}$; $\log\frac{aMg^{++}}{a^2H^+} = 0{,}2 \log K + 0{,}4 \log\frac{aNa^+}{aH^+}$
10	$2{,}33Al_2Si_2O_5(OH)_4 + 2{,}68SiO_2 + 0{,}66Na^+ \rightleftarrows 2Na_{0,33}Al_{2,33}Si_{3,67}O_{10}(OH)_2 + 2{,}33H_2O + 0{,}66H^+$ $\log K = -\frac{2461}{T} + 3{,}232 - 0{,}022\frac{(P-1)}{T}$; $\log\frac{aNa^+}{aH^+} = 1{,}515 \log K$
11	$Na_{0,33}Al_{2,33}Si_{3,67}O_{10}(OH)_2 + 2Na^+ + 3{,}32SiO_2 \rightleftarrows 2H^+ + 2{,}33NaAlSi_3O_8$ $\log K = -\frac{3862}{T} - 1{,}688 - 0{,}161\frac{(P-1)}{T}$; $\log\frac{aNa^+}{aH^+} = -0{,}5 \log K$
12	$2{,}33Al_2Si_2O_5(OH)_4 + 0{,}33Mg^{++} + 2{,}68SiO_2 \rightleftarrows 2Mg_{0,167}Al_{2,33}Si_{3,67}O_{10}(OH)_2 + 0{,}66H^+ + 2{,}33H_2O$ $\log K = -\frac{3554}{T} + 7{,}516 - 0{,}079\frac{(P-1)}{T}$; $\log\frac{aMg^{++}}{a^2H^+} = -3{,}03 \log K$
13	$2Mg_{0,167}Al_{2,33}Si_{3,67}O_{10}(OH)_2 + 11{,}316Mg^{++} + 18{,}64H_2O \rightleftarrows 2{,}33Mg_5Al_2Si_3O_{10}(OH)_8 + 22{,}632H^+ + 0{,}35SiO_2$ $\log K = -\frac{358973}{T} + 42{,}339 + 0{,}532\frac{(P-1)}{T}$; $\log\frac{aMg^{++}}{a^2H^+} = -0{,}088 \log K$

Table 2. (Continued).

No.	reaction; log K; log $\frac{{}^{a}Me^{+n}}{a^{n}_{H+}}$
14	$Na_{0,33}Al_{2,33}Si_{3,67}O_{10}(OH)_2 + 0{,}167Mg^{++} \rightleftarrows Mg_{0,167}Al_{2,33}Si_{3,67}O_{10}(OH)_2 + 0{,}33Na^+$ $\text{Log K} = -\frac{568}{T} + 2{,}187 - 0{,}028\frac{(P-1)}{T}; \log\frac{{}^{a}Mg^{++}}{a^2H^+} = -5{,}988 \log K + 1{,}976 \log\frac{{}^{a}Na^+}{{}^{a}H^+}$
15	$KAl_3Si_3O_{10}(OH)_2 + 3Na^+ + 6SiO_2 \rightleftarrows 3NaAlSi_3O_8 + K^+ + 2H^+$ $\text{Log K} = -\frac{5744}{T} + 0{,}605 - 0{,}125\frac{(P-1)}{T}; \log\frac{{}^{a}K^+}{{}^{a}H^+} = \log K + 3\log\frac{{}^{a}Na^+}{{}^{a}H^+}$
16	$2{,}33NaAlSi_3O_8 + 0{,}167Mg^{++} + 2H^+ \rightleftarrows Mg_{0,167}Al_{2,33}Si_{3,67}O_{10}(OH)_2 + 2{,}33Na^+ + 3{,}32SiO_2$ $\text{Log K} = \frac{3294}{T} + 3{,}875 + 0{,}133\frac{(P-1)}{T}; \log\frac{{}^{a}Mg^{++}}{a^2H^+} = -5{,}988 \log K + 13{,}952 \log\frac{{}^{a}Na^+}{{}^{a}H^+}$
17	$KAl_3Si_3O_{10}(OH)_2 + 6SiO_2 + 2K^+ \rightleftarrows 3KAlSi_3O_8 + 2H^+$ $\text{Log K} = -\frac{1370}{T} - 5{,}113 - \frac{0{,}258\ (P-1)}{T}; \log\frac{{}^{a}K^+}{{}^{a}H^+} = -0{,}5 \log K$
18	$1{,}5Al_2Si_2O_5(OH)_4 + K^+ \rightleftarrows KAl_3Si_3O_{10}(OH)_2 + 1{,}5H_2O + H^+$ $\text{Log K} = -\frac{812}{T} - 0{,}696 - \frac{0{,}097\ (P-1)}{T}; \log\frac{{}^{a}K^+}{{}^{a}H^+} = -\log K$
19	$1{,}5Al_2Si_2O_5(OH)_4 + Na^+ \rightleftarrows NaAl_3Si_3O_{10}(OH)_2 + 1{,}5H_2O + H^+$ $\text{Log K} = -\frac{2475}{T} + 0{,}99 - 0{,}054\frac{(P-1)}{T}; \log\frac{{}^{a}Na^+}{{}^{a}H^+} = -\log K$
20	$2{,}33\ KAlSi_3O_8 + 0{,}33Na^+ + 2H^+ \rightleftarrows Na_{0,33}Al_{2,33}Si_{3,67}\ O_{10}(OH)_2 + 2{,}33K^+ + 3{,}32SiO_2$ $\text{Log K} = \frac{465}{T} + 6{,}129 + 0{,}264\frac{(P-1)}{T}; \log\frac{{}^{a}Na^+}{{}^{a}H^+} = -3{,}03 \log K + 7{,}061 \log\frac{{}^{a}K^+}{{}^{a}H^+}$
21	$2{,}33KAl_3Si_3O_{10}(OH)_2 + 0{,}99Na^+ + 4{,}02SiO_2 + 1{,}34H^+ \rightleftarrows 2{,}33K^+ + 3Na_{0,33}Al_{2,33}Si_{3,67}O_{10}(OH)_2$ $\text{Log K} = -\frac{1799}{T} + 6{,}47 + 0{,}192\frac{(P-1)}{T}; \log\frac{{}^{a}Na^+}{{}^{a}H^+} = -1{,}01 \log K + 2{,}353 \log\frac{{}^{a}K^+}{{}^{a}H^+}$
22	$2{,}33KAlSi_3O_8 + 0{,}167Mg^{++} + 2H^+ \rightleftarrows Mg_{0,167}Al_{2,33}Si_{3,67}O_{10}(OH)_2 + 2{,}33K^+ + 3{,}32SiO_2$ $\text{Log K} = -\frac{119}{T} + 8{,}333 + 0{,}236\frac{(P-1)}{T}; \log\frac{{}^{a}Mg^{++}}{a^2H^+} = -5{,}988 \log K + 13{,}952 \log\frac{{}^{a}K^+}{{}^{a}H^+}$
23	$2{,}33KAl_3Si_3O_{10}(OH)_2 + 4{,}02SiO_2 + 0{,}501Mg^{++} + 1{,}34H^+ \rightleftarrows 3Mg_{0,167}Al_{2,33}Si_{3,67}O_{10}(OH)_2 + 2{,}33K^+$ $\text{Log K} = -\frac{3539}{T} + 13{,}072 + 0{,}107\frac{(P-1)}{T}; \log\frac{{}^{a}Mg^{++}}{a^2H^+} = -2 \log K + 4{,}65 \log\frac{{}^{a}K^+}{{}^{a}H^+}$
24	$K_{0,33}Al_{2,33}Si_{3,67}O_{10}(OH)_2 + 0{,}167Mg^{++} \rightleftarrows Mg_{0,167}Al_{2,33}Si_{3,67}O_{10}(OH)_2 + 0{,}33K^+$ $\text{Log K} = -\frac{543}{T} + 1{,}553 + 0{,}107\frac{(P-1)}{T}; \log\frac{{}^{a}Mg^{++}}{a^2H^+} = -5{,}988 \log K + 1{,}976 \log\frac{{}^{a}K^+}{{}^{a}H^+}$
25	$2{,}33Al_2Si_2O_5(OH)_2 + 0{,}66K^+ + 2{,}68SiO_2 \rightleftarrows 2K_{0,33}Al_{2,33}Si_{3,67}O_{10}(OH)_2 + 2{,}33H_2O + 0{,}66H^+$ $\text{Log K} = -\frac{2508}{T} + 4{,}499 - 0{,}294\frac{(P-1)}{T}; \log\frac{{}^{a}K^+}{{}^{a}H^+} = -1{,}515 \log K$
26	$3K_{0,33}Al_{2,33}Si_{3,67}O_{10}(OH)_2 + 1{,}34K^+ \rightleftarrows 2{,}33KAl_3Si_3O_{10}(OH)_2 + 4{,}02\ SiO_2 + 1{,}34H^+$ $\text{Log K} = \frac{1870}{T} - 8{,}373 + 0{,}215\frac{(P-1)}{T}; \log\frac{{}^{a}K^+}{{}^{a}H^+} = -0{,}746 \log K$

Table 2. (Continued).

No.	reaction; $\log K$; $\log \frac{{}^{a}Me^{+n}}{a^{n}_{H+}}$
27	$K_{0,33}Al_{2,33}Si_{3,67}O_{10}(OH)_2 + 0{,}33Na^+ \rightleftarrows Na_{0,33}Al_{2,33}Si_{3,67}O_{10}(OH)_2 + 0{,}33K^+$ $\log K = \frac{23}{T} - 0{,}634 + 0{,}136\frac{(P-1)}{T}$; $\log\frac{{}^{a}Na^+}{{}^{a}H^+} = -3{,}03\log K + \log\frac{{}^{a}K^+}{{}^{a}H^+}$
28	$K_{0,33}Al_{2,33}Si_{3,67}O_{10}(OH)_2 + 2K^+ + 3{,}32SiO_2 \rightleftarrows 2{,}33\,KAlSi_3O_8 + 2H^+$ $\log K = -\frac{442}{T} - 6{,}742 - 0{,}129\frac{(P-1)}{T}$; $\log\frac{{}^{a}K^+}{{}^{a}H^+} = -0{,}5\log K$
29	$NaAl_3Si_3O_{10}(OH)_2 + 6SiO_2 + 2Na^+ \rightleftarrows 3NaAlSi_3O_8 + 2H^+$ $\log K = -\frac{4083}{T} - 1{,}083 - \frac{0{,}168\,(P-1)}{T}$; $\log\frac{{}^{a}Na^+}{{}^{a}H^+} = -0{,}5\log K$
30	$Na_{0,33}Al_{2,33}Si_{3,67}O_{10}(OH)_2 + 2Na^+ + 3{,}32SiO_2 \rightleftarrows 2{,}33NaAlSi_3O_8 + 2H^+$ $\log K = -\frac{5201}{T} + 0{,}268 - 0{,}161\frac{(P-1)}{T}$; $\log\frac{{}^{a}Na^+}{{}^{a}H^+} = -0{,}5\log K$
31	$KAl_3Si_3O_{10}(OH)_2 + Na^+ \rightleftarrows NaAl_3Si_3O_{10}(OH)_2 + K^+$ $\log K = -\frac{1663}{T} + 1{,}686 + 0{,}043\frac{(P-1)}{T}$; $\log\frac{{}^{a}K^+}{{}^{a}H^+} = \log K + \log\frac{{}^{a}Na^+}{{}^{a}H^+}$
32	$3Na_{0,33}Al_{2,33}Si_{3,67}O_{10}(OH)_2 + 1{,}34Na^+ \rightleftarrows 4{,}02\,SiO_2 + 1{,}34H^+ + 2{,}33NaAl_3Si_3O_{10}(OH)_2$ $\log K = -\frac{2075}{T} - 2{,}542 - 0{,}092\frac{(P-1)}{T}$; $\log\frac{{}^{a}Na^+}{{}^{a}K^+} = -0{,}746\log K$
33	$2KAl_3Si_3O_{10}(OH)_2 + 15Mg^{++} + 3SiO_2 + 24H_2O \rightleftarrows 3Mg_5Al_2Si_3O_{10}(OH)_8 + 2K^+ + 28H^+$ $\log K = -\frac{78993}{T} + 65{,}757 + 0{,}776\frac{(P-1)}{T}$; $\log\frac{{}^{a}K^+}{{}^{a}H^+} = 0{,}5\log K + 7{,}5\log\frac{{}^{a}Mg^{++}}{a^2H^+}$
34	$2NaAl_3Si_3O_{10}(OH)_2 + 15Mg^{++} + 3SiO_2 + 24H_2O \rightleftarrows 3Mg_5Al_2Si_3O_{10}(OH)_8 + 2Na^+ + 28H^+$ $\log K = -\frac{75519}{T} + 62{,}23 + 0{,}691\frac{(P-1)}{T}$; $\log\frac{{}^{a}Na^+}{{}^{a}H^+} = 0{,}5\log K + 7{,}5\log\frac{{}^{a}Mg^{++}}{a^2H^+}$
35	$2{,}33NaAl_3Si_3O_{10}(OH)_2 + 0{,}501Mg^{++} + 4{,}02\,SiO_2 + 1{,}34H^+ \rightleftarrows 3Mg_{0,167}Al_{2,33}Si_{3,67}O_{10}(OH)_2 + 2{,}33Na^+$ $\log K = -\frac{384}{T} - 9{,}097 + 0{,}007\frac{(P-1)}{T}$; $\log\frac{{}^{a}Mg^{++}}{a^2H^+} = 1{,}996\log K + 4{,}66\log\frac{{}^{a}Na^+}{{}^{a}H^+}$
36	$K_{0,33}Al_{2,33}Si_{3,67}O_{10}(OH)_2 + 2{,}33Na^+ + 3{,}32SiO_2 \rightleftarrows 0{,}33K^+ + 2H^+ + 2{,}33NaAlSi_3O_8$ $\log K = -\frac{3839}{T} - 2{,}322 - 0{,}025\frac{(P-1)}{T}$; $\log\frac{{}^{a}K^+}{{}^{a}H^+} = 3{,}03\log K + 7{,}06\log\frac{{}^{a}Na^+}{{}^{a}H^+}$
37	$3K_{0,33}Al_{2,33}Si_{3,67}O_{10}(OH)_2 + 2{,}33Na^+ \rightleftarrows 2{,}33NaAl_3Si_3O_{10}(OH)_2 + 0{,}99K^+ + 4{,}02SiO_2 + 1{,}34H^+$ $\log K = -\frac{2004}{T} - 4{,}442 + 0{,}314\frac{(P-1)}{T}$; $\log\frac{{}^{a}K^+}{{}^{a}H^+} = 1{,}01\log K + 2{,}353\log\frac{{}^{a}Na^+}{{}^{a}H^+}$
38	$Al_2Si_2O_5(OH)_4 + 6Mg^{++} + 4SiO_2 + 2K^+ + 7H_2O \rightleftarrows 2KMg_3AlSi_3O_{10}(OH)_2 + 14H^+$ $\log K = -\frac{31657}{T} + 21{,}094 + 0{,}091\frac{(P-1)}{T}$; $\log\frac{{}^{a}Mg^{++}}{a^2H^+} = -0{,}167\log K - 0{,}333\log\frac{{}^{a}K^+}{{}^{a}H^+}$
39	$Mg_{0,167}Al_{2,33}Si_{3,67}O_{10}(OH)_2 + 2{,}33K^+ + 6{,}823Mg^{++} + 3{,}32SiO_2 + 9{,}32H_2O \rightleftarrows 2{,}33KMg_3AlSi_3O_{10}(OH)_2 + 15{,}98H^+$ $\log K = -\frac{35082}{T} + 20{,}772 + 0{,}146\frac{(P-1)}{T}$; $\log\frac{{}^{a}Mg^{++}}{a^2H^+} = -0{,}147\log K - 0{,}341\log\frac{{}^{a}K^+}{{}^{a}H^+}$

Table 2. (Continued).

No.	reaction; $\log K$; $\log \frac{a_{Me^{+n}}}{a^n_{H+}}$
40	$2KMg_3AlSi_3O_{10}(OH)_2 + 4H^+ \rightleftarrows Mg_5Al_2Si_3O_{10}(OH)_8 + 2K^+ + Mg^{++} + 3SiO_2$ $\log K = \frac{4834}{T} + 0{,}309 + 0{,}103\ \frac{(P-1)}{T}; \log \frac{a_{Mg^{++}}}{a^2_{H^+}} = \log K - 2 \log \frac{a_{K^+}}{a_{H^+}}$
41	$KAl_3Si_3O_{10}(OH)_2 + 9Mg^{++} + 2K^+ + 6SiO_2 + 12H_2O \rightleftarrows 3KMg_3AlSi_3O_{10}(OH)_2 + 2OH^+$ $\log K = -\frac{46673}{T} + 32{,}312 + 0{,}233\ \frac{(P-1)}{T}; \log \frac{a_{Mg^{++}}}{a^2_{H^+}} + -0{,}111 \log K - 0{,}222 \log \frac{a_{K^+}}{a_{H^+}}$
42	$KAlSi_3O_8 + 3Mg^{++} + 4H_2O \rightleftarrows KMg_3AlSi_3O_{10}(OH)_2 + 6H^+$ $\log K = -\frac{15101}{T} + 12{,}475 + 0{,}164\ \frac{(P-1)}{T}; \log \frac{a_{Mg^{++}}}{a^2_{H^+}} = -0{,}333 \log K$
43	$NaAlSi_3O_8 + K^+ + 3Mg^{++} + 4H_2O \rightleftarrows KMg_3AlSi_3O_{10}(OH)_2 + Na^+ + 6H^+$ $\log K = -\frac{13668}{T} + 10{,}604 + 0{,}119\ \frac{(P-1)}{T}; \log \frac{a_{Na^+}}{a_{H^+}} = \log K + 3 \log \frac{a_{Mg^{++}}}{a^2_{H^+}} + \log \frac{a_{K^+}}{a_{H^+}}$
44	$KAl_3Si_3O_{10}(OH)_2 + Na_{0{,}33}Al_{2{,}33}Si_{3{,}67}O_{10}(OH)_2 + 0{,}382Mg^{++} + 1{,}727SiO_2 + 0{,}576H^+ \rightleftarrows 2{,}288Mg_{0{,}167}Al_{2{,}33}Si_{3{,}67}O_{10}(OH)_2 + K^+ + 0{,}33Na^+$ $\log K = -\frac{2067}{T} + 7{,}761 + 0{,}017\ \frac{(P-1)}{T}; \log \frac{a_{Na^+}}{a_{H^+}} = 3{,}03 \log K - 3{,}03 \log \frac{a_{K^+}}{a_{H^+}} + 1{,}158 \log \frac{a_{Mg^{++}}}{a^2_{H^+}}$
45	$1{,}717Mg_{0{,}167}Al_{2{,}33}Si_{3{,}67}O_{10}(OH)_2 + Na^+ + K^+ + 2{,}713Mg^{++} + 4H_2O \rightleftarrows NaAl_3Si_3O_{10}(OH)_2 + 0{,}301SiO_2 + KMg_3AlSi_3O_{10}(OH)_2$ $\log K = -\frac{15994}{T} + 7{,}585 + 0{,}060\ \frac{(P-1)}{T}; \log \frac{a_{Na^+}}{a_{H^+}} = -\log K - \log \frac{a_{K^+}}{a_{H^+}} - 2{,}713 \log \frac{a_{Mg^{++}}}{a^2_{H^+}}$
46	$2Al_2Si_2O_5(OH)_4 + 2SiO_2 + Na^+ + K^+ + 3Mg^{++} + 2H_2O \rightleftarrows NaAl_3Si_3O_{10}(OH)_2 + KMg_3AlSi_3O_{10}(OH)_2 + 8H^+$ $\log K = -\frac{19085}{T} + 14{,}121 - 0{,}008\ \frac{(P-1)}{T}; \log \frac{a_{Na^+}}{a_{H^+}} = -\log K - \log \frac{a_{K^+}}{a_{H^+}} - 3 \log \frac{a_{Mg^{++}}}{a^2_{H^+}}$
47	$NaAl_3Si_3O_{10}(OH)_2 + 2K^+ + 6Mg^{++} + 6SiO_2 + 8H_2O \rightleftarrows NaAlSi_3O_8 + 2KMg_3AlSi_3O_{10}(OH)_2 + 14H^+$ $\log K = -\frac{30900}{T} + 18{,}405 + 0{,}071\ \frac{(P-1)}{T}; \log \frac{a_{K^+}}{a_{H^+}} = -0{,}5 \log K - 3 \log \frac{a_{Mg^{++}}}{a^2_{H^+}}$
48	$2KAl_3Si_3O_{10}(OH)_2 + K^+ + 9Mg^{++} + Na^+ + 6SiO_2 + 12H_2O \rightleftarrows NaAl_3Si_3O_{10}(OH)_2 + 3KMg_3AlSi_3O_{10}(OH)_2 + 20H^+$ $\log K = -\frac{49087}{T} + 36{,}568 + 0{,}276\ \frac{(P-1)}{T}; \log \frac{a_{Na^+}}{a_{H^+}} = -\log K - \log \frac{a_{K^+}}{a_{H^+}} - 9 \log \frac{a_{Mg^{++}}}{a^2_{H^+}}$
49	$KAl_3Si_3O_{10}(OH)_2 + K^+ + Na^+ + 6Mg^{++} + 6SiO_2 + 8H_2O \rightleftarrows NaAlSi_3O_8 + 2KMg_3AlSi_3O_{10}(OH)_2 + 2H^+$ $\log K = -\frac{33005}{T} + 21{,}708 + 0{,}114\ \frac{(P-1)}{T}; \log \frac{a_{Na^+}}{a_{H^+}} = -\log K - \log \frac{a_{K^+}}{a_{H^+}} - 6 \log \frac{a_{Mg^{++}}}{a^2_{H^+}}$
50	$Mg_{0{,}167}Al_{2{,}33}Si_{3{,}67}O_{10}(OH)_2 + 3{,}82Mg^{++} + 1{,}33K^+ + 3{,}32SiO_2 + Na^+ + 5{,}32H_2O \rightleftarrows NaAlSi_3O_8 + 9{,}98H^+ + 1{,}33KMg_3AlSi_3O_{10}(OH)_2 + 9{,}98H^+$ $\log K = -\frac{21451}{T} + 10{,}206 + 0{,}026\ \frac{(P-1)}{T}; \log \frac{a_{Na^+}}{a_{H^+}} = -\log K - 3{,}82 \log \frac{a_{Mg^{++}}}{a^2_{H^+}} - 1{,}33 \log \frac{a_{K^+}}{a_{H^+}}$
51	$Na_{0{,}33}Al_{2{,}33}Si_{3{,}67}O_{10}(OH)_2 + K_{0{,}33}Al_{2{,}33}Si_{3{,}67}O_{10}(OH)_2 + 0{,}334Mg^{++} \rightleftarrows 0{,}33Na^+ + 0{,}33K^+ + 2Mg_{0{,}167}Al_{2{,}33}Si_{3{,}67}O_{10}(OH)_2$ $\log K = -\frac{1113}{T} + 3{,}74 + 0{,}079\ \frac{(P-1)}{T}; \log \frac{a_{Na^+}}{a_{H^+}} = 3{,}03 \log K + 1{,}012 \log \frac{a_{Mg^{++}}}{a^2_{H^+}} - \log \frac{a_{K^+}}{a_{H^+}}$

Table 2. (Continued).

No.	reaction; log K; log $\frac{a Me^{+n}}{a^n_{H+}}$
52	$1{,}429K_{0{,}33}Al_{2{,}33}Si_{3{,}67}O_{10}(OH)_2 + Na^+ + 0{,}167Mg^{++} + 1{,}423SiO_2 \rightleftarrows NaAlSi_3O_8 + 0{,}858H^+ + Mg_{0{,}167}Al_{2{,}33}Si_{3{,}67}O_{10}(OH)_2$ $\log K = -\frac{2193}{T} + 0{,}556 + 0{,}096\frac{(P-1)}{T}; \log\frac{a Na^+}{a H^+} = -\log K - 0{,}167\log\frac{a Mg^{++}}{a^2H^+} + 0{,}172\log\frac{a K^+}{a H^+}$
53	$3{,}33KAlSi_3O_8 + Na^+ + 0{,}167Mg^{++} + 2H^+ \rightleftarrows NaAlSi_3O_8 + Mg_{0{,}167}Al_{2{,}33}Si_{3{,}67}O_{10}(OH)_2 + 3{,}33K^+ + 3{,}32SiO_2$ $\log K = -\frac{1561}{T} + 10{,}19 + 0{,}281\frac{(P-1)}{T}; \log\frac{a Na^+}{a H^+} = -\log K - 0{,}167\log\frac{a Mg^{++}}{a^2H^+} + 3{,}33\log\frac{a K^+}{a H^+}$
54	$KAl_3Si_3O_{10}(OH)_2 + NaAl_3Si_3O_{10}(OH)_2 + 0{,}43Mg^{++} + 1{,}15H^+ + 3{,}45SiO_2 \rightleftarrows Na^+ + K^+ + 2{,}575Mg_{0{,}167}Al_{2{,}33}Si_{3{,}67}O_{10}(OH)_2$ $\log K = -\frac{1347}{T} + 9{,}501 + 0{,}049\frac{(P-1)}{T}; \log\frac{a Na^+}{a H^+} = \log K + 0{,}43\log\frac{a Mg^{++}}{a^2H^+} - \log\frac{a K^+}{a H^+}$
55	$KAl_3Si_3O_{10}(OH)_2 + NaAlSi_3O_8 + 0{,}287Mg^{++} + 0{,}301SiO_2 + 1{,}434H^+ \rightleftarrows K^+ + Na^+ + 1{,}717Mg_{0{,}167}Al_{2{,}33}Si_{3{,}67}O_{10}(OH)_2$ $\log K = -\frac{134}{T} + 7{,}29 + 0{,}102\frac{(P-1)}{T}; \log\frac{a Na^+}{a H^+} = \log K + 0{,}287\log\frac{a Mg^{++}}{a^2H^+} - \log\frac{a K^+}{a H^+}$

1965; Helgeson, 1968, 1970). The work of Helgeson et al. (1969) further represents a brief review of the more fundamental relationships.

Both 2 and 3-dimensional figures are presented here, not only for clarity, but also to show the mutual relationships of ratios of activities in isothermal and isobaric conditions (also for the other pressures than 1 bar when the diagrams are redrawn including the pressure term of the log K expression).

Among the most important advantages of both the reactions and the diagrams are that they provide:

1. an opportunity to calculate the parameters related to intersections, or to the range of values of parameters along boundary surfaces of coexisting minerals,
2. localization of points expressing the chemical composition of natural solutions and defining the pathways of change of their associated parameters, and
3. determination of the changes in the stability fields of minerals with respect to T and p, and the prediction of the limits of these parameters in a given process, so that geological models can be realistically constrained.

Insight into the advantages of these points may be gained by comparing the following examples with the corresponding number 1–3 above:

1. the intersection of lines 23, 17, 42 yields the values p = 1 b, t≈513 K, and p = 1 kb, T≈559K. These levels indicate the end of a stable coexistence of phlogopite and muscovite in the aqueous solution. For 472 K and p = 1 b the upper limit of phlogopite, muscovite and K-feldspar coexistence in an aqueous solution is described by:

$$\log a_{Mg}{}^{++}/a_H^{2+} = 6.48;\ \log a_K{}^+/a_H{}^+ = 4;$$
$$\log a_{Na}{}^+/a_H{}^+ = 5.18$$

and exist along boundary line resulting from the intersection of the three planes.

2. When the primary influence of T on the activity of sea water components is considered the changes of some their basic parameters can be summarized (Table 3). These values mark the probable pathway of sea water evolution in activity diagrams. Such a change of parameters, supplemented by a discussion of the water/rock ratios, could be very helpful for an understanding of the hydrothermal alteration processes caused by solutions originating from sea water.
3. Tracing the changes of the stability area of mus-

Table 3. Basic cationic composition of sea water and its physico-chemical characteristic in various T and P = 0,5 kb.

T (K)	Ionic strength	pH*	log H_2CO_3***	Log Na^+***	m_Na+*	log $\frac{a_{Na^+}}{a_{H^+}}$	log K^+**	m_{K+}*	log $\frac{a_{K^+}}{a_{H^+}}$	log Mg^{++}**	mMg^{++}	log $\frac{a_{Mg^{++}}}{a^2_{H^+}}$
298	0,67	7,63	0,0722	−0,1165	0,45	7,17	−0,1586	0,0097	5,46	−0,4573	0,0511	13,51
333	0,67	7,70	0,0622	−0,1384	0,45	7,21	−0,1836	0,0097	5,50	−0,4990	0,0504	13,60
373	0,67	7,23	0,0546	−0,1633	0,45	6,72	−0,2130	0,0097	5,00	−0,5531	0,0504	12,61
423	0,67	6,43	0,0520	−0,1938	0,45	5,89	−0,2509	0,0097	4,17	−0,6309	0,0504	10,93
473	0,64	6,20	0,0596	−0,2210	0,45	5,63	−0,2866	0,0097	3,9	−0,7186	0,0510	10,39
523	0,63	5,80	0,0843	−0,2489	0,45	5,20	−0,3281	0,0097	3,46	−0,8361	0,0506	9,47
573	0,60	3,01	0,1139	−0,3054	0,45	2,36	−0,4065	0,0097	0,59	−1,040	0,0438	3,616
623	0,59	2,52	0,2700***	−0,3459	0,45	1,83	−0,4991	0,0097	0,01	−1,412	0,0402	2,244

* Values after Bischoff and Seyfried (1978).
** The delta approximation (Helgeson, 1970).
*** Extrapolation to 623K.
**** After Helgeson (1969).

covite with T and p (lines 26, 17) provides the level at which the muscovite in an aqueous solution ends, namely for p = 1 b, at T = 564 K, and for p = 1 kb, at T = 642 K.

Discussion

Refering to Figs 1a–8a, increasing temperature does not greatly affect the log a_{K^+}/a_{H^+} at which microcline alters to muscovite or clay. On the other hand the log $a_{Mg^{++}}/a^2_{H^+}$ at which microline alteres to pholopite or Mg-chlorite drops from 13 to about 4, with increasing T. At the same time the stability fields of muscovite and kaolinite decrease while that of montmorillonite increases. The behaviour of albite in the Na analogue system (Figs 1b–8b) parallels that in the K-system. Increasing temperature causes the log a_{Na^+}/a_{H^+} at which albite reacts to form paragonite or clay to drop from about 7.5 to 4. Phlogopite can only form from albite at values of log $a_{Na^+}/a_{H^+}>12$. Looking at the interaction of the alkalies in terms of log a_{Na^+}/a_{H^+} and log a_{K^+}/a_{H^+} (Figs 1c–8c), increasing temperature affects albite relatively more than microcline. Apart from the albitization of microcline, no direct alteration of K-feldspar to Na mica or clay is possible. Figs 9–12 combine the data of Figs 1 to 8 to produce 3-dimensional projections showing the stability volumes of the mineral phases described above in terms of log a_{Na^+}/a_{H^+}, log a_{K^+}/a_{H^+} and log $a_{Mg^{++}}/a^2_{H^+}$. These graphical representations enable on the one hand, realistic alteration trends to be predicted, and on the other hand those parageneses already found can be used to gain information on the PTX conditions operating during hydrothermal alteration. With increasing T the stability volume of phlogolite, and to a lesser extent Mg-chlorite, expands at the expense of the feldspars, micas and clays. Kaolinite, with a large stability volume at low T is almost excluded at higher temperatures, decreasing at the expense of montmorillonite. Similarly paragonite has a very restricted stability volume, and muscovite is not stable in this projection above 573 K.

The value of these diagrams in giving a greater understanding to the widespread alteration processes known to have been operating in the 1.9–1.86 Ga felsis supracrustals of W. Bergslagen still has to be evaluated. Phlogopite is a common mineral in many of the hydrothermal alteration zones (eg. Linthout, 1983; Baker & De Groot, 1983; Trägårdh, 1988). Calculations presented here show that phlogopite, stable at 298 K, increases in stabil-

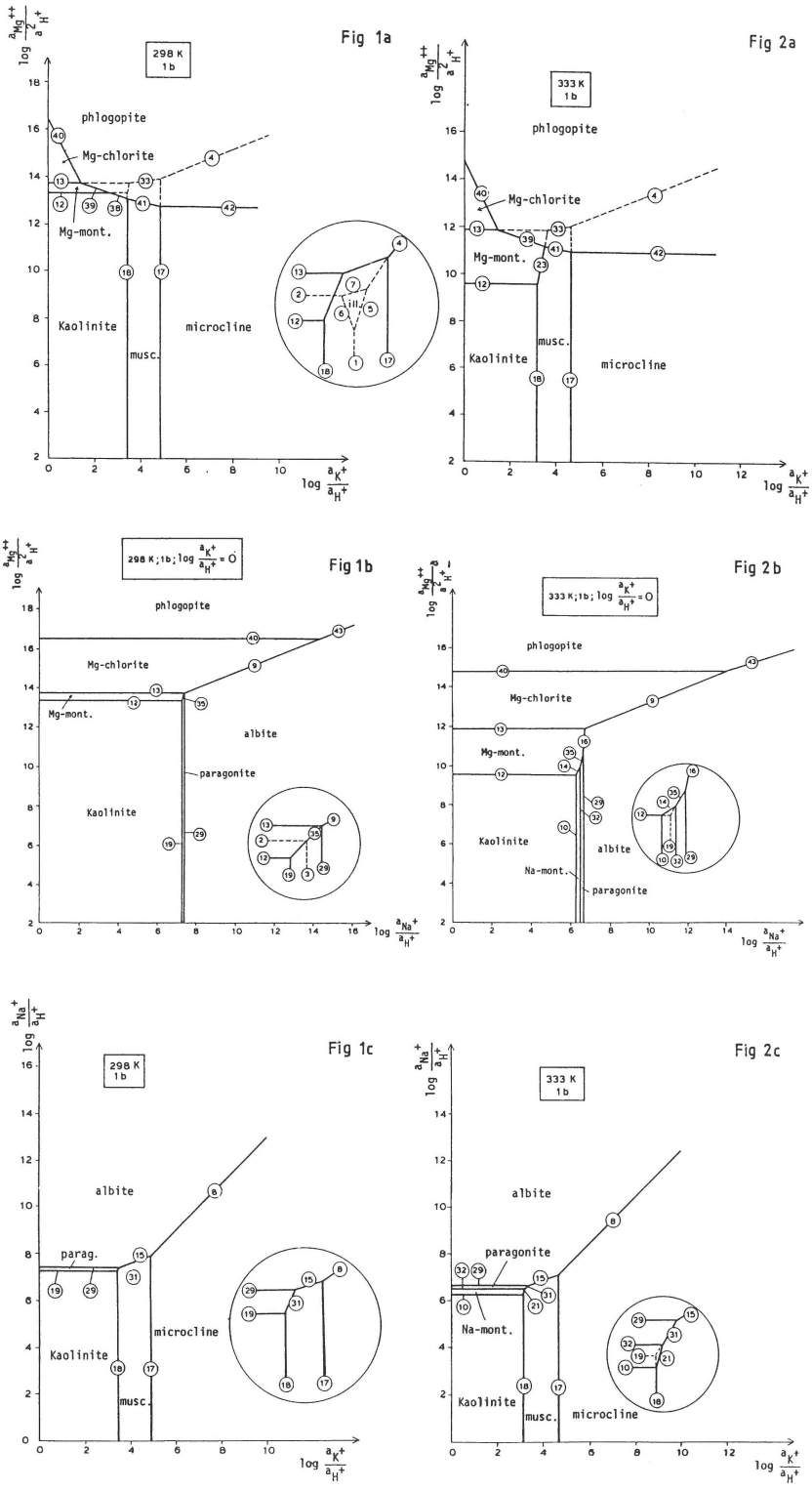

Figs 1a–8a: Log a_{Mg++}/a^2_{H+} versus log a_{K+}/a_{H+} for the MgO-Al_2O_3-Na_2O-K_2O-H_2O-HCl system, for 1 bar and temperatures from 298–623 K, showing the effects of increasing T on the stability fields of phlogopite, Mg-chlorite, muscovite, microcline, Mg- and K-montmorillonite and kaolinite.

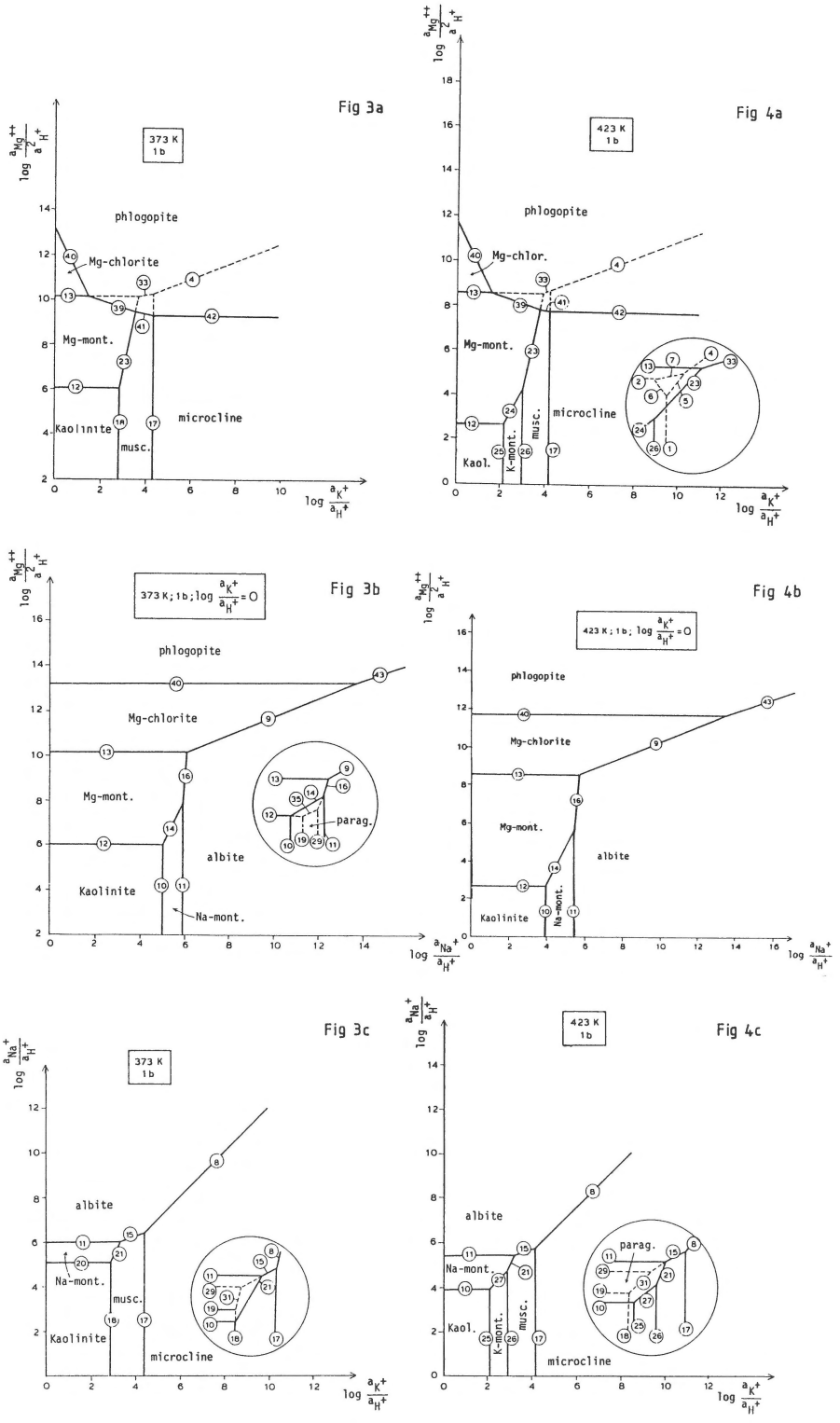

Figs 1b–8b: Log $a_{Mg^{++}}/a^2_{H+}$ versus log a_{Na+}/a_{H+} for the MgO-Al_2O_3-Na_2O-K_2O-H_2O-HCl system, for 1 bar and temperatures from 298–623 K, showing the effects of increasing T on the stability fields of phlogopite, Mg-chlorite, paragonite, albite, Mg- and Na-montmorillonite and kaolinite.

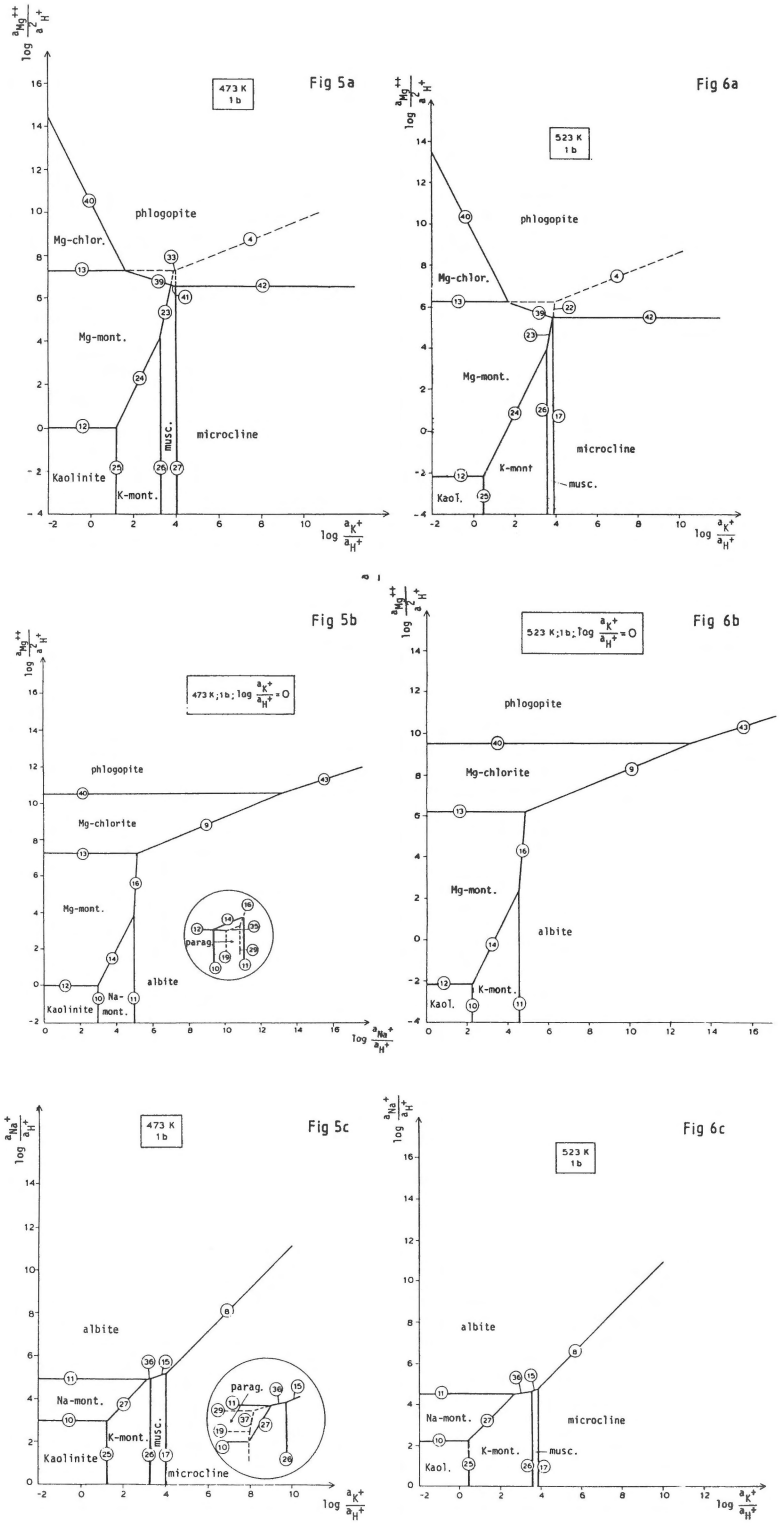

Figs 1c–8c: Log a_{Na+}/a_{H+} versus log a_{K+}/a_{H+} for the MgO-Al_2O_3-Na_2O-K_2O-H_2O-HCl system, for 1 bar and temperature from 298–623 K, showing the effects of increasing T on the stability fields of microcline, albite, muscovite, paragonite, Na- and K-montmorillonite and kaolinite.

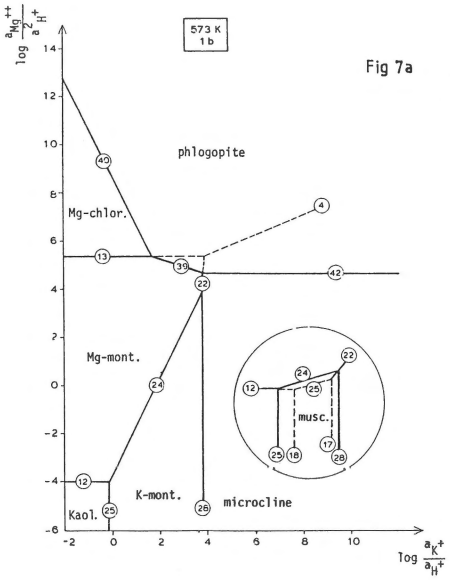

Fig 7a

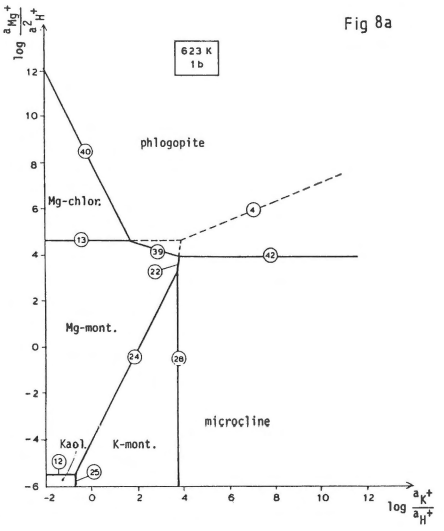

Fig 8a

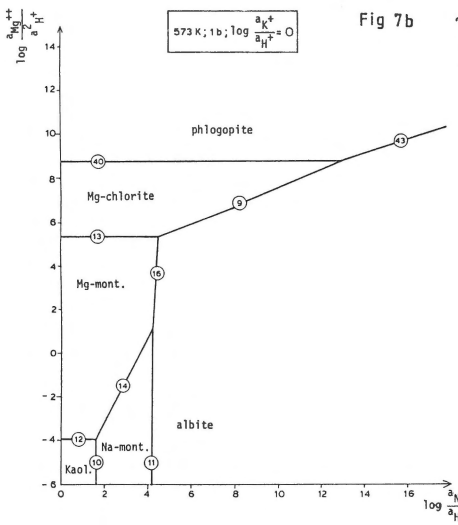

Fig 7b

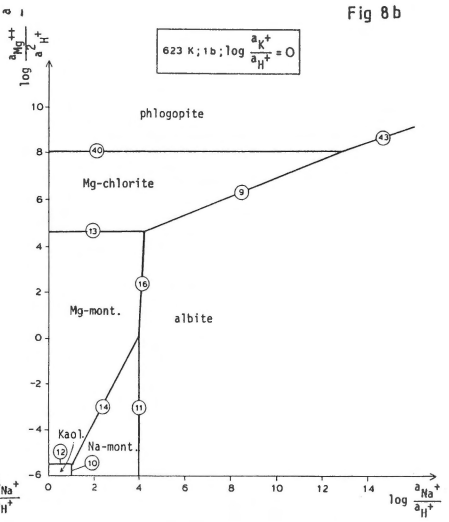

Fig 8b

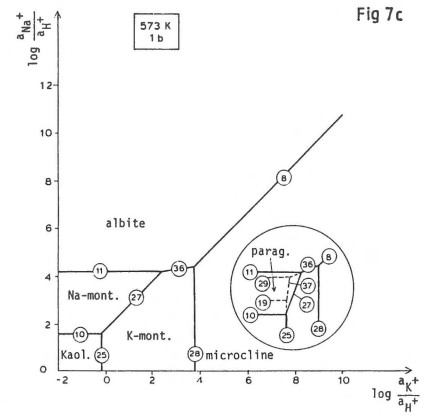

Fig 7c

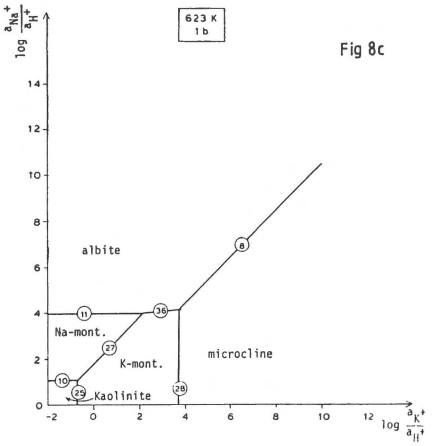

Fig 8c

(for figure legend see pp 387–389)

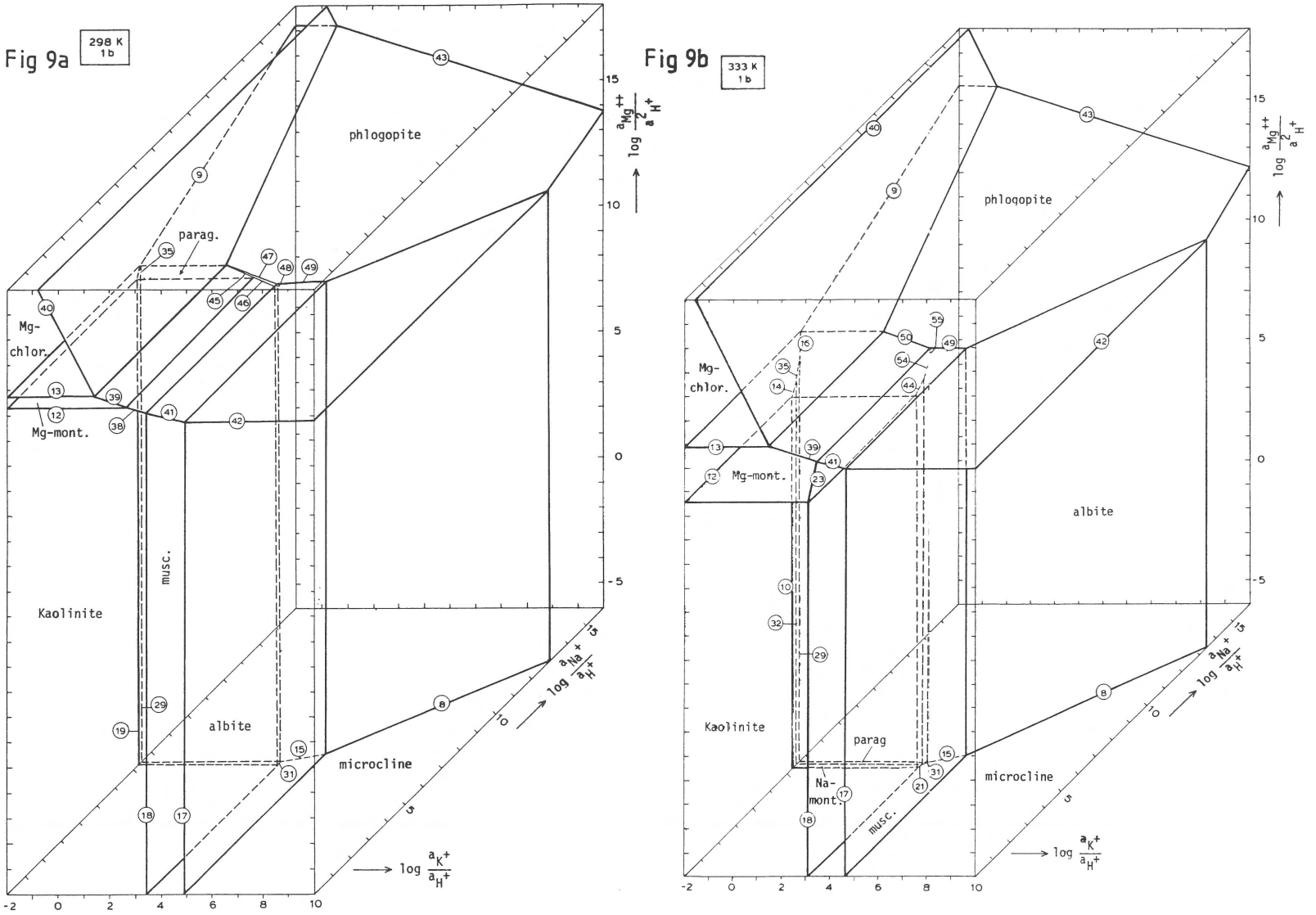

Fig. 9. Block diagram of log a_{Mg++}/a^2_{H+}, log a_{Na+}/a_{H+}, and log a_{K+}/a_{H+} for the MgO-Al_2O_3-Na_2O-K_2O-H_2O-HCl system at 1 bar and temperatures from 298–623 K, showing the stability volumes of phlogopite, Mg-chlorite, muscovite, paragonite, microcline, albite, Mg-, K-, and Na-montmorillonite and kaolin.

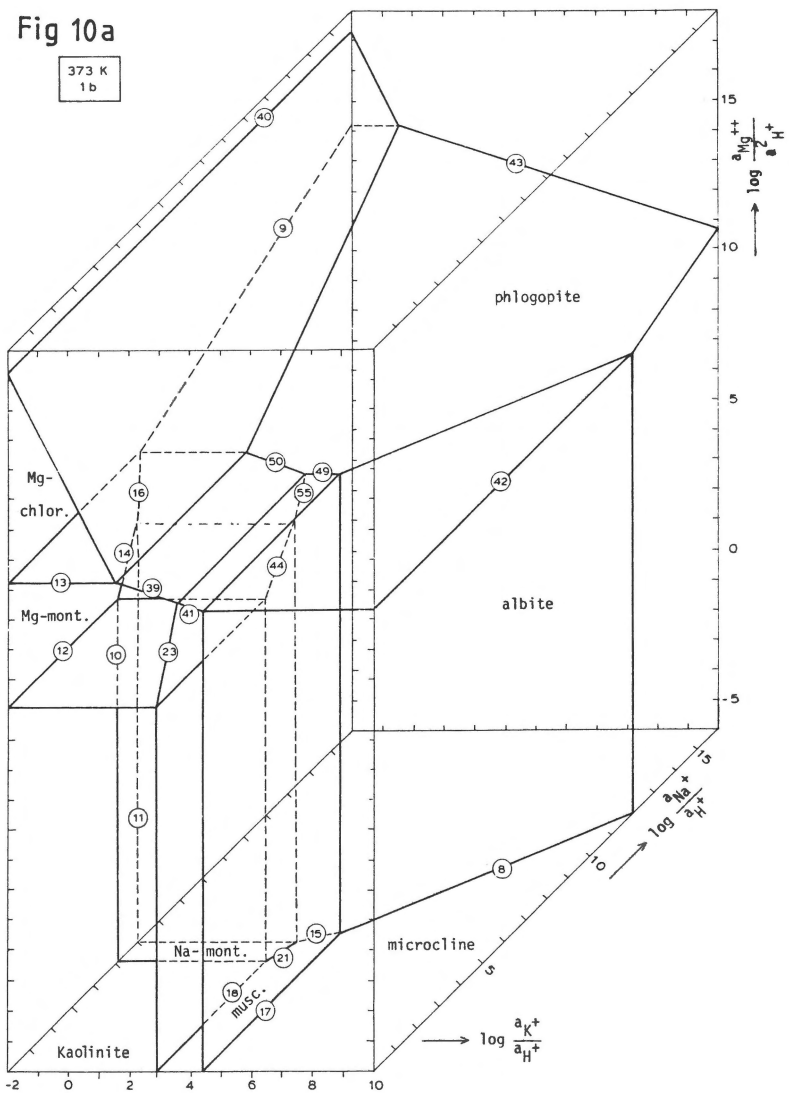

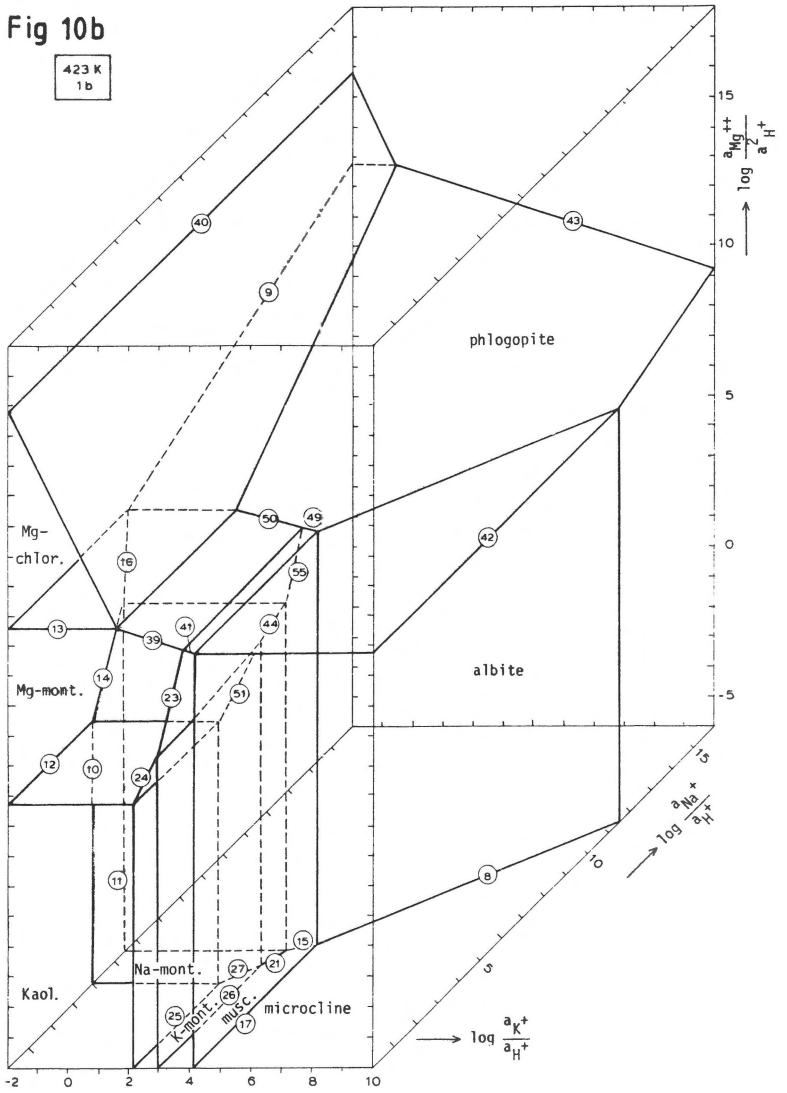

Fig. 10. Block diagram of log a_{Mg++}/a^2_{H+}, log a_{Na+}/a_{H+}, and log a_{K+}/a_{H+} for the MgO-Al_2O_3-Na_2O-K_2O-H_2O-HCl system at 1 bar and temperatures from 298–623 K, showing the stability volumes of phlogopite, Mg-chlorite, muscovite, paragonite, microcline, albite, Mg-, K-, and Na-montmorillonite and kaolin.

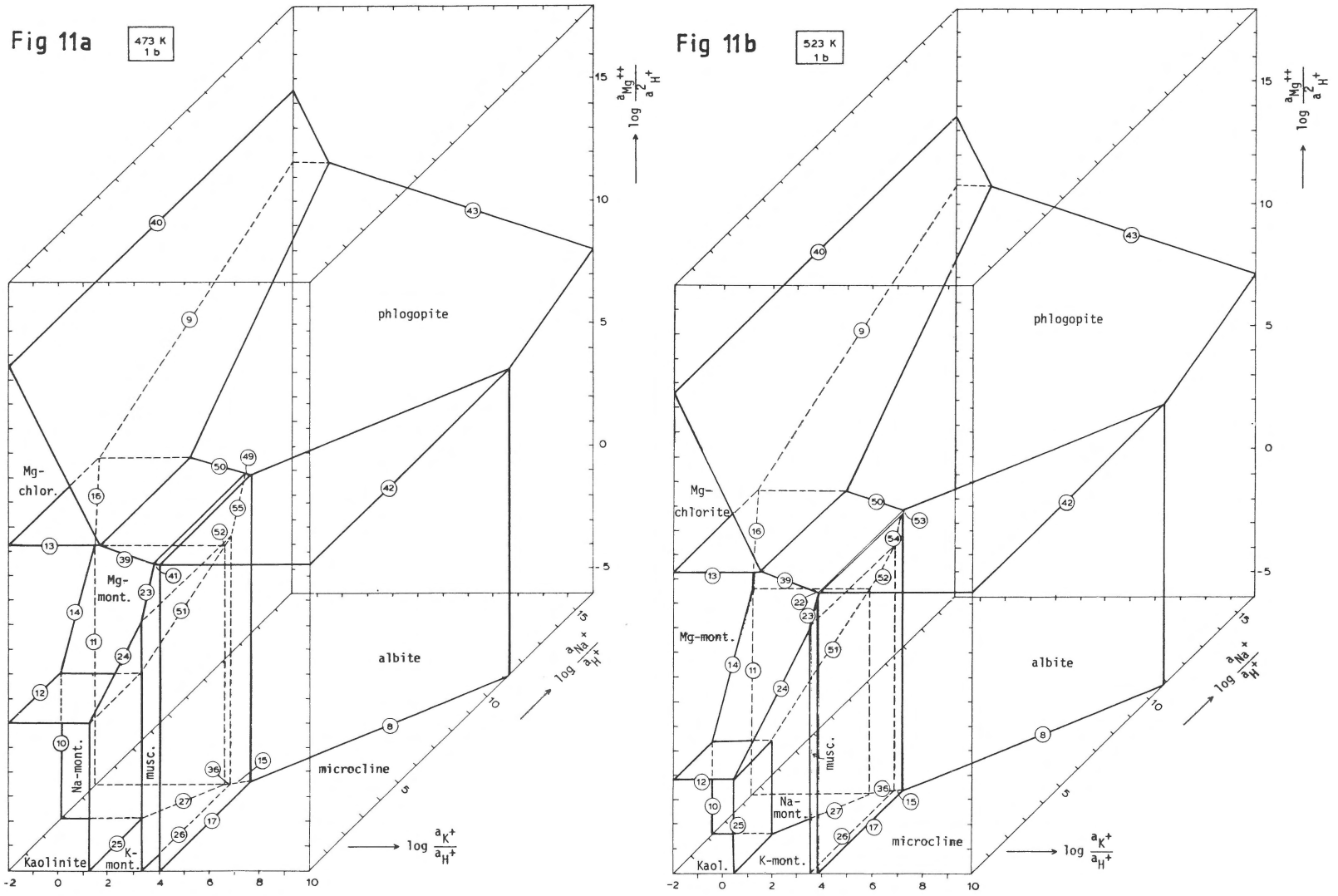

Fig. 11. Block diagram of log $a_{Mg^{++}}/a^2_{H^+}$, log a_{Na^+}/a_{H^+}, and log a_{K^+}/a_{H^+} for the MgO-Al_2O_3-Na_2O-K_2O-H_2O-HCl system at 1 bar and temperatures from 298–623 K, showing the stability volumes of phlogopite, Mg-chlorite, muscovite, paragonite, microcline, albite, Mg-, K-, and Na-montmorillonite and kaolin.

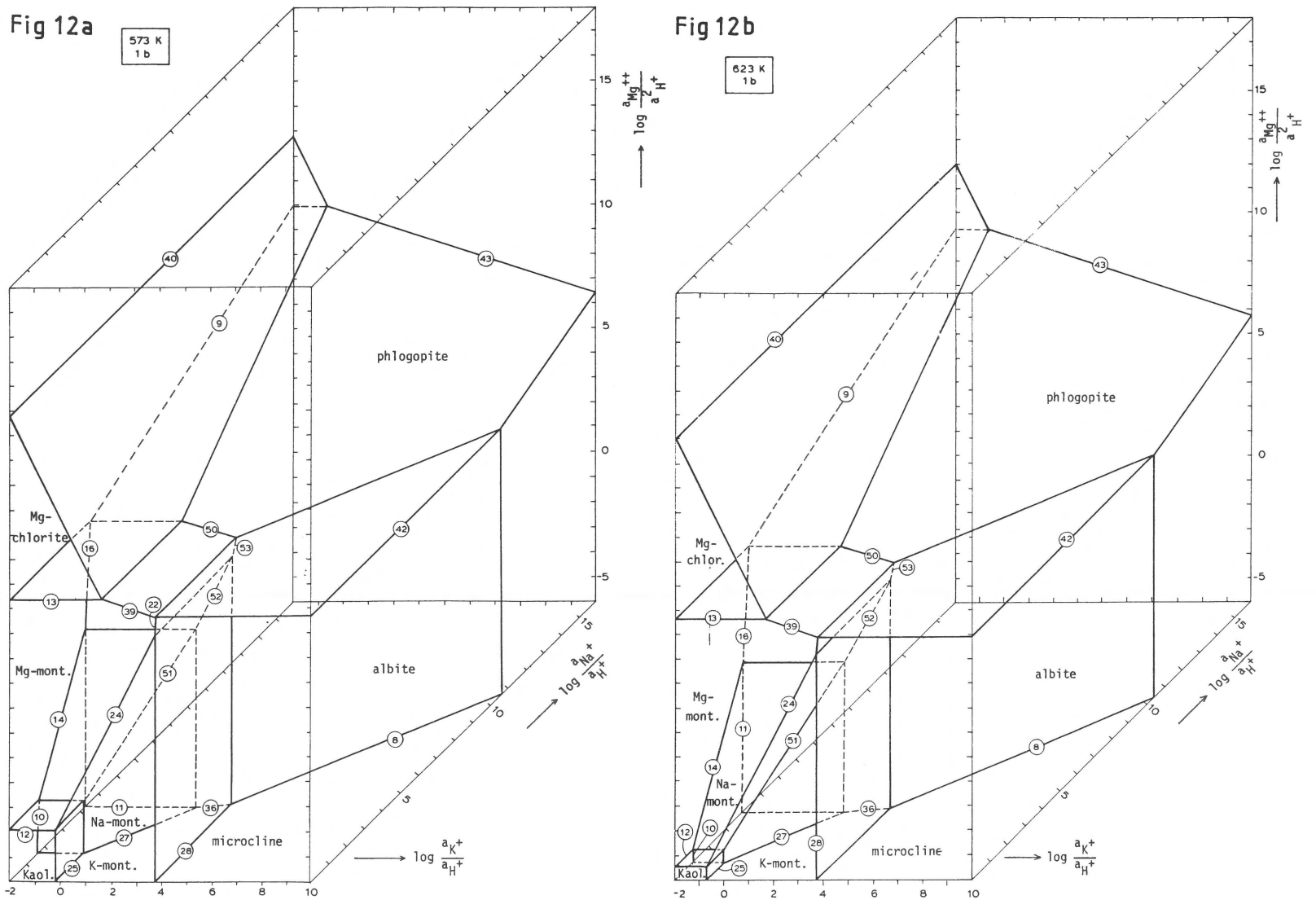

Fig. 12. Block diagram of log $a_{Mg^{++}}/a^2_{H^+}$, log a_{Na^+}/a_{H^+}, and log a_{K^+}/a_{H^+} for the MgO-Al_2O_3-Na_2O-K_2O-H_2O-HCl system at 1 bar and temperatures from 298–623 K, showing the stability volumes of phlogopite, Mg-chlorite, muscovite, paragonite, microcline, albite, Mg-, K-, and Na-montmorillonite and kaolin.

ity with increasing T up to 623 K, under a realistic range of geological conditions.

Acknowledgements

I wish to thank K. Linthout and Dr. J.H. Baker for their assistance and stimulation, and Prof J. Touret for valuable discussions. I also acknowledge the assistance of F. Kievits, H.A. Sion, G.B. Snijder and C. van der Bliek in the preparation of this paper.

References

Baker, J.H. & De Groot, P.A. 1983 Proterozoic seawater-felsic volcanics interaction, W. Bergslagen, Sweden. Evidence for high REE mobility and implications for 1.8 Ga seawater compositions – Contrib. Mineral. Petrol. 82: 119–130

Frietsch, R. 1982 Alkalimetasomatism and the ore-bearing metavolcanics of central Sweden – Sver. Geol. Unders. C791: 1–54

Garrels, R.M. & Christ, C.L. 1965 Solution, minerals and equilibria – Harper & Row: 450 pp

Helgeson, H.C. 1968 Evaluation of irreversible reactions in geochemical processes involving minerals and aqueous solutions – I. Thermodynamic relations – Geochim. Cosmochim. Acta 32: 853–877

Helgeson, H.C., Brown, T.H. & Leeper R.H. 1969 Handbook of theoretical activity diagrams depicting chemical equilibria in geologic system involving an aqueous phase at one atm and 0° to 3000° C – Freeman, Cooper & Cy: 253 pp

Helgeson, H.C. 1970 Solution chemistry and metamorphism. In: P.H. Abelson (ed.): Researches in geochemistry II – John Wiley: 362–404

Helgeson, H.C., Delany, J.M., Nesbitt, H.W. & Bird, D.K. 1978 Summary and critique of the thermodynamic properties of rock forming minerals – Am. J. Sci 278-A: 229 pp

Jasiński, A.W., Baker, J.H. & De Groot, P.A. 1985 Thermodynamic aspects of the Mg-chlorite – alkali feldspar – sericite-kaolinite system: Applications to the fossil sub-seafloor hydrothermal system at Hjulsjö, Bergslagen, Sweden – GUA Papers of Geology, ser. 1, 21

Lagerblad, B & Gorbatschev, R. 1985 Hydrothermal alteration as a control of regional geochemistry and ore formation in the Central Baltic Shield – Geol. Rundsch. 74: 33–49

Linthout, K. 1983 From rhyolites to quartz-phlogopite-muscovite schist: Proterozoic two-stage sub-seafloor alteration. W. Bergslagen. Central Sweden. (Abstract) – Terra Cognita

Oen, I.S. 1987 Rift-related igneous activity and metallogenesis in S.W. Bergslagen, Sweden – Precambr. Res. 35: 367–382

Oen, I.S., Helmers, H., Verschure, R.H. & Wiklander, U 1982 Ore deposition in a Proterozoic incipient rift zone environment: A tentative model for the Filipstad-Grythyttan-Hjulsjö region, Bergslagen, Sweden – Geol. Rundsch. 71: 182–194

Ripa, M. 1988 Geochemistry of wall-rock alteration and mixed volcanic-exhalative facies at the Proterozoic Stollberg Fe-Pb-Zn-Mn-(-Ag) deposit, Bergslagen, Sweden – In: Baker, J.H. & Hellingwerf, R.H. (eds): The Bergslagen Province, Central Sweden – Structure, stratigraphy and ore-forming processes. I.G.C.P. project 247. Geol. Mijnbouw 67: 443–457(this issue).

Robie, R.A., Hemingway, B.S. & Fisher, J.R. 1978 Thermodynamic properties of minerals and related substances at 298.15 K and 1 bar (10^5 Pascals) pressure and at higher temperatures – U.S. Geol. Surv. Bull. 1452: 456

Tardy, Y. & Garrels, R.M. 1974 A method of estimating the Gibbs energies of formation of layer silicates – Geochim. Cosmochim. Acta 38: 1101–1116

Trägårdh, J. 1988 Cordierite-mica-quartz schists in a Proterozoic volcanic iron-ore bearing terrain, Riddarhyttan area, Bergslagen, Sweden – In: Baker, J.H. & Hellingwerf, R.H. (eds): The Bergslagen Province, Central Sweden – Structure, stratigraphy and ore-forming processes. I.G.C.P. project 247. Geol. Mijnbouw 67: 397–409 (this issue)